HETEROCYCLES, Vol. 98, No. 11, 2019, pp. 1513 - 1524. © 2019 The Japan Institute of Heterocyclic Chemistry
Received, 9th October, 2019, Accepted, 1st November, 2019, Published online, 6th November, 2019
DOI: 10.3987/COM-19-14167

# A HIGHLY SELECTIVE FLUORESCENCE-ENHANCED PROBE FOR THE RAPID DETECTION OF $SO_2$ DERIVATIVES AND ITS BIO-IMAGING IN LIVING CELLS

**Yaogen Zhou, Yiwei Zhou, Hongying Wang,* and Baoquan Chen***

Tianjin Key Laboratory of Organic Solar Cells and Photochemical Conversion, School of Chemistry and Chemical Engineering, Tianjin University of Technology, Tianjin 300384, P. R. China; E-mail: hywang243@126.com (H. Wang); chenbaoquan66@126.com (B. Chen)

**Abstract** – In this study, we report a simple coumarin-based probe **CISD** for the detection of $SO_2$ derivatives. In the case of the probe **CISD**, $HSO_3^-$ can induce an obvious fluorescence-enhanced response with high selectivity, fast response (within 10 sec) as well as low limit of detection (262 nM). HR-MS experiment revealed the sensing mechanism concerning the nucleophilic addition reaction. Furthermore, the probe **CISD** has been successfully applied for imaging exogenous $HSO_3^-$ in living HeLa cells.

## INTRODUCTION

Sulfur dioxide ($SO_2$) is a most common environmental pollutant, and inhaled $SO_2$ can be easily hydrated to sulfurous acid in the respiratory tract, followed by the formation of its derivatives, sulfite and bisulfite ($SO_3^{2-}$ and $HSO_3^-$, 3:1 M/M in neutral fluid and plasma).[1] Additionally, $SO_2$ derivatives are largely used as preservatives and additives for many drinks, foodstuffs, and pharmaceuticals due to its antimicrobial, bacteriostatic and antioxidant abilities, which make the human exposure to $SO_2$ increasingly widespread. In fact, $SO_2$ can be also endogenously produced during the normal processing of sulfur-containing amino acid in mammals,[2,3] and as a biologically active molecule, it could mediate a wide range of physiological and pathophysiological processes, e.g. having vasorelaxant effect,[4] improving myocardial antioxidant capacity,[5] ameliorating pulmonary vascular structural remodeling,[6] and regulating cardiovascular function,[7] etc. Unfortunately, as a double-edged sword, excessive intake of $SO_2$ and its derivatives could also exert very harmful influences on human health. A large number of epidemiological studies have shown that chronic or acute exposure to unregulated amounts of $SO_2$ in the human body may induce many health issues, such as asthma and allergic reactions,[8] neurological diseases,[9] and even lung cancer.[10]

To maintain homeostasis in humans, the concentration of $SO_2$ derivatives is tightly regulated. Accordingly, developing simple and highly sensitive methods for the detection and quantitation of $SO_2$ derivatives in environmental monitoring and biological applications is absolutely essential.

To date, several methods have been developed for the detection of $SO_2$ derivatives in food and environment, such as chromatography, spectrophotometry, and electrochemical analysis.[11-15] However, most of these methods depend on multiple reagents and expensive apparatus, or require complex pre-treatment processes and time-consuming work. Fluorescent probes as an important class of promising technique, have revolutionized our ability to detect and monitor analytes in real-time with excellent selectivity, sensitivity and reproducibility, convenient operating system, high spatial and temporal resolution as well as non-invasiveness and non-destructiveness.[16-18] Additionally, probes can also serve the concomitant visualization of distinct analytes and processes.[19] In this context, the development of fluorescent probes for the detection of $SO_2$ derivatives represents a very active research field, and many small molecule fluorescence probes with different $SO_3^{2-}/HSO_3^-$-reactive moiety like aldehyde, double bond and levulinate have been developed.[20-26] Nevertheless, there are still some limitations for $SO_2$ probes, e.g. long response time, interference from hydrogen sulfide ($H_2S$), as well as high range of organic cosolvents.[27] Thus, further study is urgently needed to develop practical and efficient sensors for sensing $SO_2$ derivatives.

Coumarins belong to benzopyrone chemical class and have been considered as promising building blocks for the construction of functional fluorescent probes due to its relatively high quantum yield, high photostability and biological compatibility.[28,29] In this work, we proposed a new coumarin-based fluorescent probe **CISD** for the detection of $SO_2$ derivatives. As shown in Scheme 1, **CISD** was constructed by the aldol condensation of 3-acetylcoumarin (**1**) and 2-methylindole-3-carboxaldehyde (**2**). Owing to the strong nucleophilicity of $SO_2$ derivatives, when the probe **CISD** is exposed to $HSO_3^-$, $HSO_3^-$ can easily attack the C=C bond linking the coumarin and 2-methylindole units in aqueous solution,[30] which could cause the change of the electronic distribution and the interruption of the π-conjugation,[24] thus leading to a significant fluorescence enhancement and a color change.

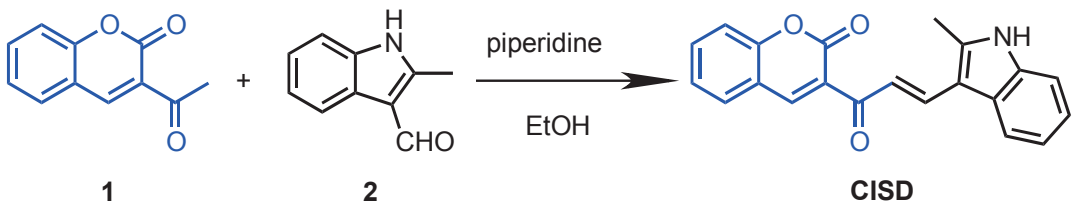


**1** **2** **CISD**

**Scheme 1.** Synthetic route of the probe **CISD**

This probe exhibits excellent sensitivity and fast response (within 10 sec) for $HSO_3^-$ with a low limit of detection. Furthermore, CCK-8 assay and cell imaging indicate that **CISD** is cell membrane permeable with low toxicity and capable of imaging of $HSO_3^-$ in living cells.

## RESULTS AND DISCUSSION

**Synthesis and Structural Characterization of CISD.** As outlined in Scheme 1, the target probe **CISD** was easily synthesized by the aldol condensation of 3-acetylcoumarin (**1**) and 2-methylindole-3-carboxaldehyde (**2**) in EtOH with piperidine as the catalyst. We employed Sephadex LH-20 column chromatography, a highly efficient separation method depending mostly on the molecular size,[31] to afford the pure compound. Its chemical structure was characterized by $^1$H NMR, $^{13}$C NMR and HR-MS (shown in the Electronic Supplementary Information Figure S1-S3). To further confirm the structure, we have performed the X-ray single crystal analysis (Figure 1). All details concerning the crystal structure are listed in Tables S1-S3.

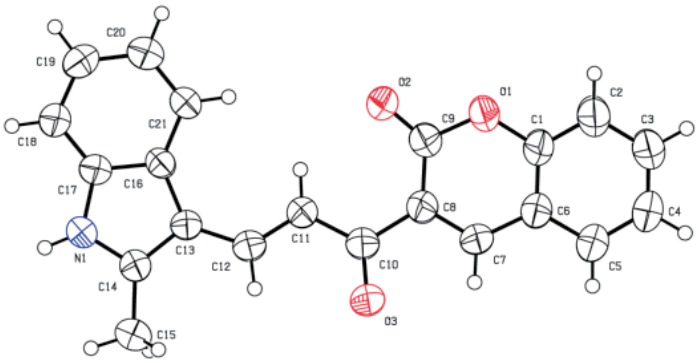


**Figure 1.** X-ray diffraction pattern of the probe **CISD**

**Spectral Responses of CISD toward $HSO_3^-$.** The sensing behavior of **CISD** (10 μM) for $HSO_3^-$ was preliminarily tested in DMSO/PBS buffer solution (v/v = 3/7, pH 7.4) at room temperature. The related probe **CISD** solution exhibited yellowish color and was essentially non-fluorescent. Upon addition 26 equiv. of $HSO_3^-$, the yellowish color of **CISD** solution immediately changed to colorless and bright green fluorescence can be observed under the irradiation of a 365 UV lamp (Figure 2 inset). Encouraged by these results, the UV–vis absorption and fluorescence emission spectra titrations of **CISD** with $HSO_3^-$ were assessed. As shown in Figure 2, the probe **CISD** exhibited a maximum absorbance peak at 435 nm and a characteristic emission at 510 nm, upon the addition of increasing amount of $HSO_3^-$ (0–260 μM), the maximum absorption wavelength at 435 nm gradually decreased with the simultaneous appearance of a new blue-shifted absorption band centered at 385 nm, which suggested that the large π-conjugation of **CISD** was interrupted by $HSO_3^-$. Meanwhile, a well-defined isosbestic point was observed at 405 nm,

indicating that **CISD** could be used as a colorimetric probe for $HSO_3^-$ through naked-eye detection method. The **CISD** itself is almost non-fluorescent in DMSO/PBS buffer solution (Φ = 0.001 with relative to fluorescein, Φr = 0.9 in 0.1 M NaOH). With increasing amount of $HSO_3^-$, the fluorescence intensity at 510 nm was gradually enhanced, and the enhancement ratio over 10-fold was triggered with the addition of 260 μM of $HSO_3^-$ (Φ = 0.015 with relative to fluorescein, Φr = 0.9 in 0.1 M NaOH). By plotting the corresponding fluorescence intensity at 510 nm *versus* the concentration of $HSO_3^-$, a good linear relationship was obtained with the concentration ranging from 0 to 80 μM ($R^2$ = 0.9994, Figure 3). Based on signal to noise ratio (S/N = 3), the detection limit of **CISD** for $HSO_3^-$ was calculated to be 262 nM. These results indicated that **CISD** could be used for quantitative detection of $HSO_3^-$ with high sensitivity.

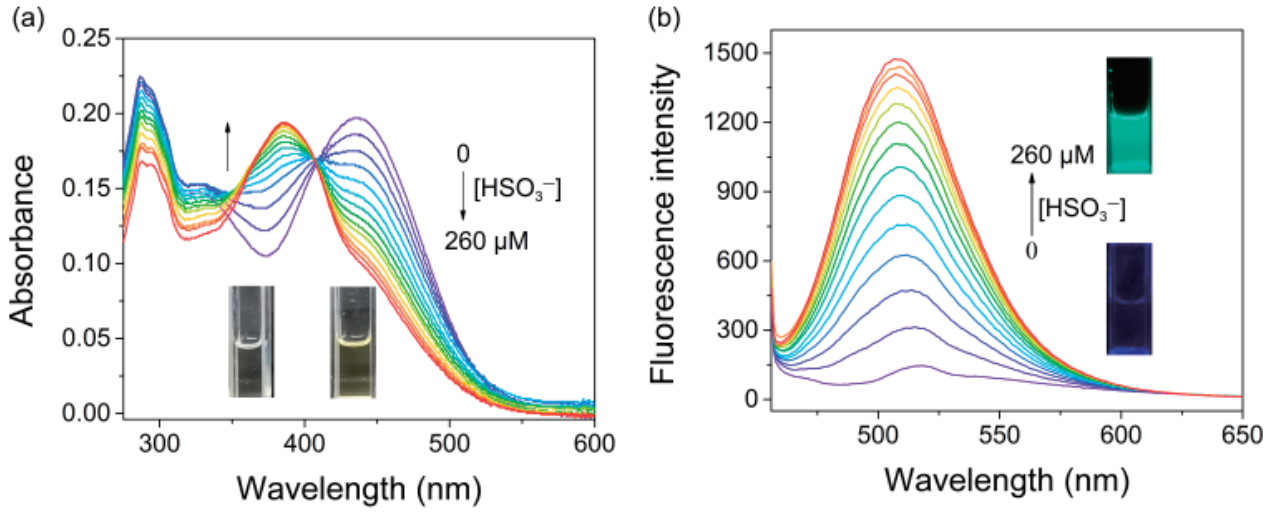


**Figure 2.** (a) UV-vis absorption and (b) fluorescence emission spectra of **CISD** (10 μM) upon the addition of increasing amount of $HSO_3^-$ (0–260 μM) in DMSO/PBS buffer solution (v/v = 3/7, pH 7.4). Inset: (a) the color and (b) fluorescence images of **CISD** in the absence/presence of $HSO_3^-$.

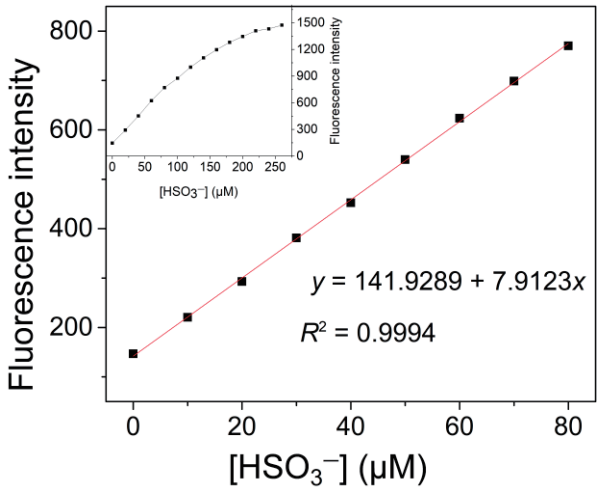


**Figure 3.** The linear relationship between the fluorescence intensity of **CISD** (10 μM) at 510 nm *versus* concentrations of $HSO_3^-$ in DMSO/PBS buffer solution (v/v = 3/7, pH 7.4)

**Selectivity Studies.** For ideal fluorescent probes, high specificity and fast response are two of the most important requirements in its practical application.[25] To evaluate the selectivity for $HSO_3^-$ /$SO_3^{2-}$, the probe **CISD** (10 μM) was treated with various potentially interference species (260 μM), especially the small molecular biothiols. As displayed in Figure 4 and Figure S4, addition of 260 μM $HSO_3^-$ /$SO_3^{2-}$ led to a noticeable fluorescence enhancement at 510 nm. By contrast, no appreciable change is observed in the presence of other species including biothiols (Hcy, Cys, and GSH), reactive oxygen species ($H_2O_2$ and $ClO^-$), metal ions ($Ca^{2+}$, $Zn^{2+}$, $Fe^{3+}$, and $Al^{3+}$), and common anions ($F^-$, $Cl^-$, $Br^-$, $I^-$, $NO_3^-$, $AcO^-$, $H_2PO_4^-$, $HPO_4^{2-}$, $S_2O_3^{2-}$, $HS^-$, $SO_4^{2-}$, and $HCO_3^-$). Thus, the probe has excellent selectivity towards $SO_2$ derivatives, which facilitates the probe to be quite suitable to track $HSO_3^-$ /$SO_3^{2-}$ in a complex system.

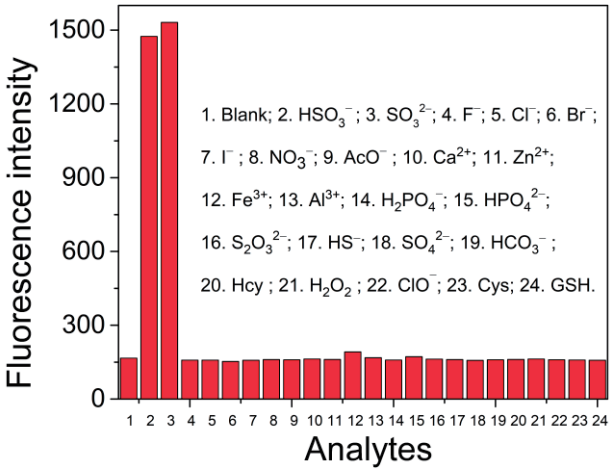


**Figure 4.** Fluorescence responses of **CISD** (10 μM) toward 260 μM of various test analytes in DMSO/PBS buffer solution (v/v = 3/7, pH 7.4) at 25 °C

**Time and pH Dependent Fluorescence Responses of CISD toward $HSO_3^-$.** The time-dependent fluorescence intensity of **CISD** toward $HSO_3^-$ was also investigated in DMSO/PBS buffer solution (v/v = 3/7, pH 7.4). As shown in Figure 5a, upon treatment of $HSO_3^-$ (260 μM), the fluorescence intensity of **CISD** (10 μM) at 510 nm increased instantly to maximum within 10 sec, which proved that **CISD** was a fast response fluorescent probe for $HSO_3^-$ and might be suitable for real-time monitoring $HSO_3^-$ levels in environment or living systems.

We subsequently evaluated the pH-dependent fluorescence responses of **CISD** (10 μM) toward $HSO_3^-$ in DMSO/PBS buffer solution (v/v = 3/7) with different pH values. As observed in Figure 5b, there was almost no obvious change from pH 4 to 10 concerning the fluorescence intensity of **CISD**, indicating that the probe itself was highly stable over a wide range of pH values. Upon the addition of $HSO_3^-$ (260 μM), the fluorescence intensity of **CISD** was significantly enhanced at the pH values ranging from 6 to 8, suggesting its potential in biological applications.

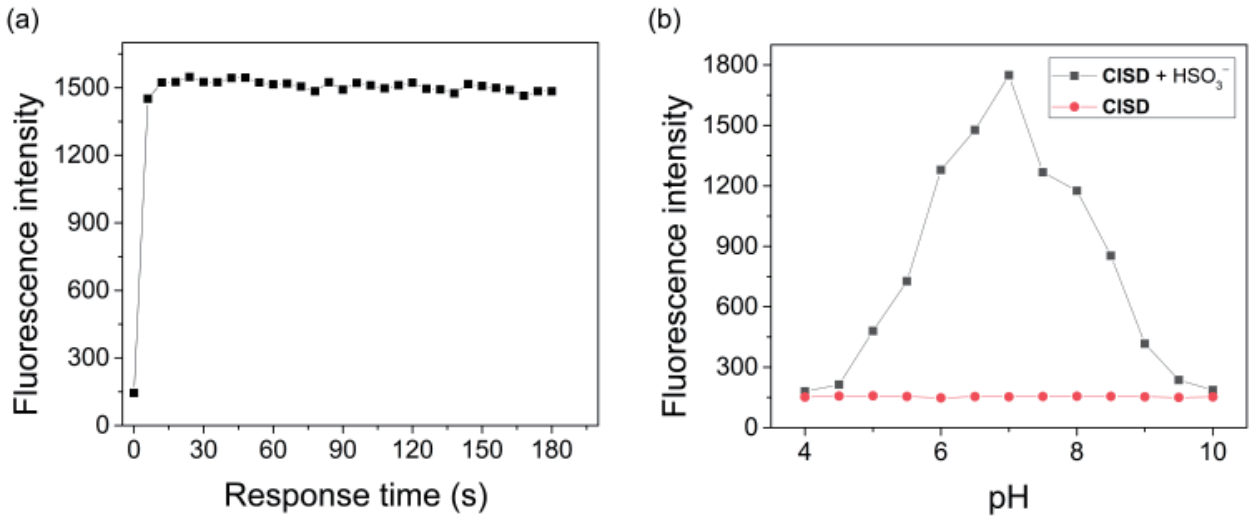


**Figure 5.** (a) Time-dependent fluorescence responses of **CISD** (10 μM) toward $HSO_3^-$ (260 μM) in DMSO/PBS buffer solution (v/v = 3/7, pH 7.4). (b) The pH-dependent fluorescence responses of **CISD** (10 μM) toward $HSO_3^-$ (260 μM) in DMSO/PBS buffer solution (v/v = 3/7) with different pH values.

**Cell Imaging.** Bearing in mind evidence on the production of $SO_2$ derivatives in cells[2], the merits of **CISD** described above, prompted us to evaluate its application for imaging $HSO_3^-$ in living cells. We first examined the cytotoxicity of **CISD** by CCK-8 assay method. Different concentrations of **CISD** (2.5, 5, 10, 15, and 20 μM) were incubated with HeLa cells for 24 h at 37 °C, and then the absorbance was measured in a plate reader at 450 nm. The cell viability results showed that the HeLa cells viability remained above 80% after incubated with 10 μM of **CISD**, clearly suggesting the probe with low toxicity under the experimental conditions (Figure 6). Subsequently, a confocal laser scanning microscope was used to investigate the ability of **CISD** for $HSO_3^-$ imaging in living cells. As expected, when HeLa cells were incubated with only probe **CISD** (10 μM) for 1 h at 37 °C, nearly non-fluorescence in green channel was observed (Figure 7a-c). After further incubation with 50 μM of $NaHSO_3$ for additional 15 min, a clear cell profile with bright green fluorescence was found (Figure 7d-f). These results indicate that **CISD** is cell membrane permeable and capable of imaging of $HSO_3^-$ in living cells.

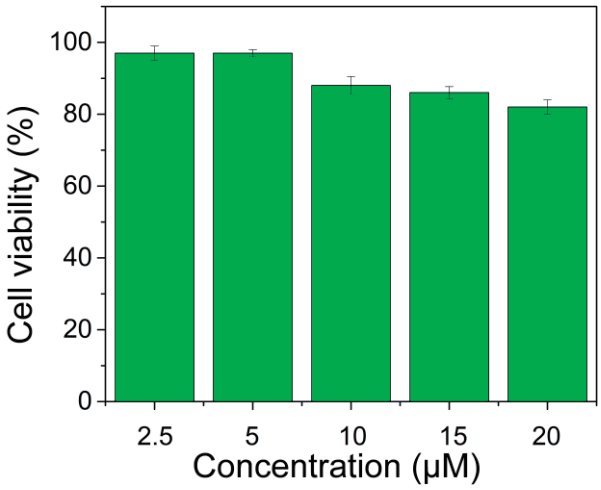


**Figure 6.** CCK-8 assay for survival rate of HeLa cells treated with different concentrations of **CISD** (2.5, 5, 10, 15, and 20 μM). Error bars are ± SD, n = 3.

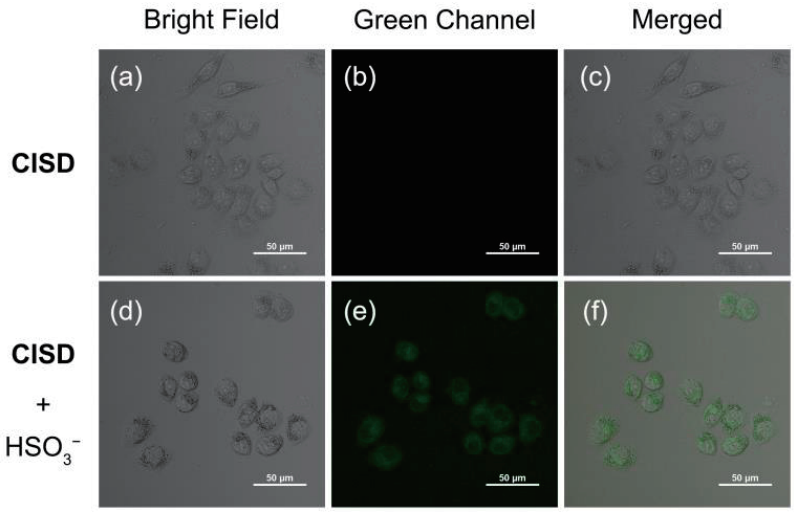


**Figure 7.** Confocal fluorescence images of HeLa cells: (a-c) the cells incubated with 10 μM of **CISD** for 1 h at 37 °C. (d-f) The cells pre-treated with 10 μM of **CISD** for 1 h, and then incubated with 50 μM of $NaHSO_3$ for 15 min. Fluorescence images of HeLa cells from green channel ($\lambda_{ex}$ = 488 nm, $\lambda_{em}$ = 500 – 530 nm). Objective lens: 40x; Scale bar: 50 μm.

**Proposed Sensing Mechanism.** It is well known that $SO_2$ derivatives, by virtue of their strong nucleophilicity, could easily attack the C=C bond of the α,β-unsaturated ketones in aqueous solution.[30] We naturally propose the sensing mechanism depicted in Scheme 2, when the probe **CISD** is exposed to $HSO_3^-$, the nucleophilic reaction of $HSO_3^-$ on the C=C bond linking the coumarin and 2-methylindole units is occurred, which can cause the change of the electronic distribution and the interruption of the π-conjugation,[24] thus leading to a significant fluorescence enhancement (from non-fluorescent to bright green) and a color change (from yellowish to colorless). To validate the sensing mechanism, HR-MS analysis was carried out. As anticipated, a noticeable signal peak at *m/z* 410.0696 observed in the HR-MS spectrum of the reaction product between **CISD** and $HSO_3^-$ (Figure S5), is corresponding to the expected

mass of the adduct product **CISD-$SO_3H$** $[M - H]^-$ (calculated: 410.0698), which confirmed the alkenyl group underwent nucleophilic addition by $HSO_3^-$.

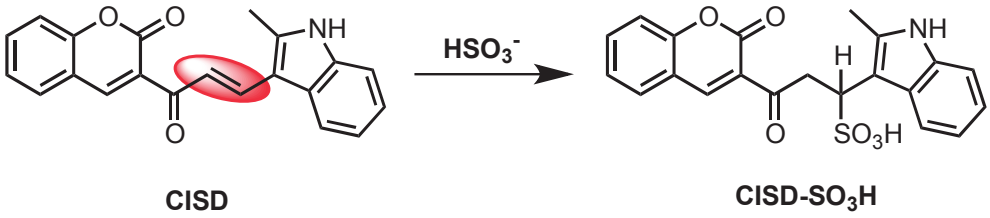


**CISD** **CISD-$SO_3H$**

**Scheme 2.** The proposed sensing mechanism of **CISD** for $HSO_3^-$

## CONCLUSIONS

In summary, we synthesized a new fluorescence probe (**CISD**) based on the aldol condensation for the detection of $SO_2$ derivatives. The probe consisted of a coumarin fluorophore with an α,β-unsaturated ketones moiety as the reaction site. Owing to the strong nucleophilicity of $SO_2$ derivatives, this probe could selectively recognize $SO_2$ derivatives based on the mechanism of nucleophilic reaction. In the case of the probe, $HSO_3^-$ induced a noticeable fluorescence-enhanced response with high selectivity and fast response (within 10 sec). In addition, **CISD** can quantitatively determine $HSO_3^-$ with a low limit of detection (262 nM). Cell staining experiments indicated that this probe can report exogenous $HSO_3^-$ in HeLa cells with remarkable fluorescence turn-on signals in the green channel. Therefore, **CISD** has a great potential application for the $SO_2$ derivatives in biological systems.

## EXPERIMENTAL

**Materials and Apparatus.** All chemicals and solvents were purchased from marketable suppliers (Aladdin-Reagent, Sigma-Aldrich, and Energy Chemical) and employed without further processing unless otherwise stated. The solvents used in spectrum analysis were all of analytical grade. Double-distilled water was used throughout the process of solution preparing and spectroscopic testing.

The reaction was performed on the magnetic stirrers and its reaction process was monitored by thin-layer chromatography (TLC) using pre-coated silica gel GF254 plates (Qingdao Haiyang Chemical Co., Ltd.) with UV indicator. The column chromatography was conducted over Sephadex LH-20 (Pharmacia). High-resolution mass spectra (HR-MS) were measured on an HP-1100 LC-MS spectrometer. NMR spectra were recorded on a Bruker AV-400 instrument ($^1H$: 400 MHz, $^{13}C$: 100 MHz), with tetramethyl-silane (TMS) as internal standard. UV-vis absorption spectra were obtained using a Hitachi UV-3310 spectrophotometer. Fluorescence spectra were generated on a Hitachi F-7000 fluorescence spectrophotometer. Cytotoxicity assays were detected by a BioTek FLx800 plate reader with Gen 5TM

software. Fluorescent images were acquired on a Nikon A1 confocal laser-scanning microscopy equipped with a live cell workstation.

**Synthesis of Probe CISD.** 2-Methylindole-3-carboxaldehyde (0.477g, 3 mmol) and 0.1 mL of piperidine were added to the solution of 3-acetylcoumarin (0.564 g, 3 mmol) in 30 mL of absolute EtOH. After stirring at 90 °C for 8 h under nitrogen atmosphere, the mixture was cooled to room temperature. Subsequently, the mixture was filtered and washed repeatedly with EtOH to give the crude product, which was further purified by Sephadex LH-20 column chromatography eluted with $CH_2Cl_2$/MeOH (1:1 v/v) to afford the probe **CISD** as a red solid (0.135 g, yield: 13%). mp 268-270 °C. $^1$H NMR (400 MHz, DMSO-$d_6$) $\delta$ (ppm) 11.95 (s, 1H), 8.68 (s, 1H), 8.04 (d, $J$ = 15.6 Hz, 1H), 7.97 (dd, $J$ = 7.5, 1.2 Hz, 1H), 7.89–7.92 (m, 1H), 7.73 (td, $J$ = 7.8, 1.2 Hz, 1H), 7.71 (d, $J$ = 15.6 Hz, 1H), 7.49 (d, $J$ = 8.4 Hz, 1H), 7.39–7.45 (m, 2H), 7.18–7.21 (m, 2H), 2.58 (s, 3H).$^{13}$C NMR (100 MHz, DMSO-$d_6$) $\delta$ (ppm) 185.42, 158.95, 154.38, 146.33, 144.91, 137.90, 136.27, 133.88, 130.35, 126.13, 125.79, 124.86, 122.31, 121.34, 119.72, 118.65, 117.20, 116.11, 111.74, 109.52, 11.91. HR-MS (ESI) *m/z* for $C_{21}H_{16}O_3N^+$ $[M + H]^+$ calculated: 330.1130; found: 330.1137.

**X-Ray Crystallographic Data Collection.** Colorless crystals of the probe **CISD** were obtained in a mixed solvent of MeOH and $CH_2Cl_2$. A suitable crystal was selected and performed on a Rigaku Rigaku SCX-MINI diffractometer at 293(2) K with MoK$\alpha$ radiation ($\lambda$ = 0.71073 Å). Using Olex2,[32] the structure was solved with the olex2.solve[33] structure solution program using Charge Flipping and refined with the olex2.refine[33,34] refinement package using Gauss-Newton minimization. Crystallographic Data: $C_{21}H_{15}NO_3$, $M$ = 329.34 g/mol: monoclinic, space group $P$ 2$_1$/c, $a$ = 6.2785(15) Å, $b$ = 27.412(5) Å, $c$ = 9.516(3) Å, $\beta$ = 102.93(3)°, $V$ = 1596.1(6) Å$^3$, $Z$ = 4, $T$ = 293(2) K, $\mu$ (MoK$\alpha$) = 0.092 mm$^{-1}$, $D_{calc}$ = 1.371 g/cm$^3$, 5102 reflections measured (5.304° ≤ 2$\theta$ ≤ 49.978°), 2816 unique ($R_{int}$ = 0.0480, $R_\sigma$ = 0.0949) which were used in all calculations. The final $R_1$ was 0.0636 ($I \geq 2\ \sigma(I)$) and $wR_2$ was 0.1835 (all data). Full crystallographic data for **CISD** can be obtained free of charge from the Cambridge Crystallographic Data Centre (deposition no. CCDC 1949582).

**General Procedure for Spectral Measurements.** Stock solutions of various test analytes (10 mM) were prepared in double-distilled water. The stock solution of probe **CISD** (1 mM) was prepared in DMSO and stored in the refrigerator before use. For spectral measurements, **CISD** was diluted to 10 μM in DMSO/PBS buffer solution (v/v = 3/7, pH 7.4), and 3.0 mL of the resulting solution was placed in a quartz cell (10-mm optical path length) each time. Fluorescence measurements were recorded with the excitation wavelength at 440 nm and the excitation slit/emission width at 5 nm/10 nm. All spectroscopic experiments were performed at room temperature in triplicate and averaged.

**Cell Viability Assay.** The cytotoxicity of **CISD** in HeLa (human cervical cancer) cells was evaluated by Cell Counting Kit-8 (CCK-8) assay. HeLa cells (Perking Union Medical College, China) were cultured in Dulbecco's modified Eagle's medium (DMEM) with 10% fetal bovine serum (FBS, Invitrogen Corp., Carlsbad, CA) and penicillin (100 units/mL)-streptomycin (100 μg/mL) antibiotics solution (Invitrogen Corp., Carlsbad, CA), and then seeded in a 96-well plastic plate ($5 \times 10^3$ cells/each well) during the exponential phase of growth. After incubation at 37 °C in a humidified $CO_2$ incubator (5% $CO_2$ and 95% air) for 24 h, the cells were washed three times with PBS. **CISD** (1 mM) was then added to the 96-well plates to give final concentrations of 2.5, 5, 10, 15 and 20 μM, respectively. After treating with probe for 24 h, the cells were washed once with PBS. Subsequently, 100 μL serum-free DMEM containing 10% CCK-8 was added to each well of the plate, and incubated for another 1 h. Finally, the absorbance was measured in a plate reader at 450 nm. The cell viability rate was calculated using the formula, described in our previously published paper.[35,36]

**Fluorescence Imaging in Living Cells.** HeLa cells were cultured in DMEM containing 10% FBS and antibiotics under standard culture environment with 5% $CO_2$ at 37 °C. The cells in exponential growth stage were seeded on uncoated 35 mm diameter glass-bottomed dishes (D110100, Matsunami, Japan) and cultured for 24 h before dye loading. Next, the culture medium was removed, and the cells were washed with PBS. In the control group, the cells were subsequently incubated with DMEM containing 10% FBS and 10 μM of **CISD** for 1 h at 37 °C, followed by washed with PBS thrice and imaged. In the experimental group, the HeLa cells were incubated with DMEM containing 10% FBS and 10 μM of **CISD** for 1 h at 37 °C, and continuously treated with 50 μM of $NaHSO_3$ for additional 15 min, washed with PBS, and then used for confocal laser-scanning microscopy measurement.

## ACKNOWLEDGEMENTS

This work was financially supported by the Natural Science Foundation of Tianjin, China (18JCQNJC75800, 18JCYBJC94900) and the National Natural Science Foundation of China (No. 31400301).

## REFERENCES

1. T. Z. Meng, G. Qin, B. Zhang, and J. Bai, *Mutagenesis*, 2004, **19**, 465.
2. T. Ubuka, S. Yuasa, J. Ohta, N. Masuoka, K. Yao, and M. Kinuta, *Acta Med. Okayama*, 1990, **44**, 55.
3. L. Luo, S. Chen, H. Jin, C. Tang, and J. Du, *Biochem. Biophys. Res. Commun.*, 2011, **415**, 61.
4. Z. Meng, Z. Yang, J. Li, and Q. Zhang, *Chemosphere*, 2012, **89**, 579.
5. H. Jin, Y. Wang, X. Wang, Y. Sun, C. Tang, and J. Du, *Nitric Oxide*, 2013, **32**, 56.

6. Y. Sun, Y. Tian, M. Prabha, D. Liu, S. Chen, R. Zhang, X. Liu, C. Tang, X. Tang, H. Jin, and J. Du, *Lab*. *Invest*., 2010, **90**, 68.
7. S. Zhang, J. Du, H. Jin, W. Li, Y. Liang, B. Geng, S. Li, C. Zhang, and C. Tang, *Transplantation*, 2009, **87**, 517.
8. T.-Y. Chiang, T.-H. Yuan, R.-H. Shie, C.-F. Chen, and C.-C. Chan, *Environ*. *Int*., 2016, **96**, 1.
9. N. Sang, Y. Yun, H. Li, L. Hou, M. Han, and G. Li, *Toxicol*. *Sci*., 2010, **114**, 226.
10. W. J. Lee, K. Teschke, T. Kauppinen, A. Andersen, P. Jäppinen, I. Szadkowska-Stanczyk, N. Pearce, B. Persson, A. Bergeret, L. A. Facchini, R. Kishi, D. Kielkowski, B. A. Rix, P. Henneberger, J. Sunyer, D. Colin, M. Kogevinas, and P. Boffetta, *Environ*. *Health Perspect.*, 2002, **110**, 991.
11. K. S. Carlos, M. Treblin, and L. S. de Jager, *Food Chem*., 2019, **286**, 537.
12. G. Leng, Q. Hu, W.-F. He, Z. Liu, W.-J. Chen, W.-B. Xu, Q.-H. Yang, and J. Sun, *J*. *Chromatogr*. *A*, 2019, **1584**, 72.
13. N. Altunay and R. Gürkan, *Anal*. *Methods*, 2016, **8**, 342.
14. N. Altunay, R. Gürkan, and K. Sertakan, *Food Anal*. *Method*, 2015, **8**, 2094.
15. Z. Daunoravicius and A. Padarauskas, *Electrophoresis*, 2002, **23**, 2439.
16. D. Wu, A. C. Sedgwick, T. Gunnlaugsson, E. U. Akkaya, J. Yoon, and T. D. James, *Chem*. *Soc*. *Rev*., 2017, **46**, 7105.
17. Y. Yue, F. Huo, F. Cheng, X. Zhu, T. Mafireyi, R. M. Strongin, and C. Yin, *Chem*. *Soc*. *Rev*., 2019, **48**, 4155.
18. P. Gao, W. Pan, N. Li, and B. Tang, *Chem*. *Sci*., 2019, **10**, 6035.
19. J. Zhang, X. Chai, X.-P. He, H.-J. Kim, J. Yoon, and H. Tian, *Chem*. *Soc*. *Rev*., 2019, **48**, 683.
20. X. Kong, J. Yin, M. Li, L. Zhu, B. Dong, Y. Ma, and W. Lin, *Sensor*. *Actuat*. *B-Chem*., 2019, **292**, 80.
21. F. Cai, B. Hou, S. Zhang, H. Chen, S. Ji, X.-c. Shen, and H. Liang, *J*. *Mater*. *Chem*. *B*, 2019, **7**, 2493.
22. Z. Ye, C. Duan, R. Sheng, J. Xu, H. Wang, and L. Zeng, *Talanta*, 2018, **176**, 389.
23. W. Zhang, F. Huo, Y. Zhang, and C. Yin, *J*. *Mater*. *Chem*. *B*, 2019, **7**, 1945.
24. J. Xu, H. Yuan, L. Zeng, and G. Bao, *Chinese Chem*. *Lett*., 2018, **29**, 1456.
25. K. Li, L.-L. Li, Q. Zhou, K.-K. Yu, J. S. Kim, and X.-Q. Yu, *Coordin*. *Chem*. *Rev*., 2019, **388**, 310.
26. H. Zhang, S. Xue, and G. Feng, *Sensor*. *Actuat*. *B-Chem*., 2016, **231**, 752.
27. D. Zhang, A. Liu, R. Ji, J. Dong, and Y. Ge, *Anal. Chim. Acta*, 2019, **1055**, 133.
28. Y. Yang, Y. Feng, Y. Jiang, F. Qiu, Y. Wang, X. Song, X. Tang, G. Zhang, and W. Liu, *Talanta*, 2019, **197**, 122.
29. H. Xu, H. Zhang, G. Liu, L. Kong, X. Zhu, X. Tian, Z. Zhang, R. Zhang, Z. Wu, Y. Tian, and H.

Zhou, *Anal*. *Chem*., 2019, **91**, 977.

30. M. Morton and H. Landfield, *J*. *Am*. *Chem*. *Soc*., 1952, **74**, 3523.
31. K. Křenek, P. Marhol, Ž. Peikerová, V. Křen, and D. Biedermann, *Food Res*. *Int*., 2014, **65**, 115.
32. O. V. Dolomanov, L. J. Bourhis, R. J. Gildea, J. A. K. Howard, and H. Puschmann, *J*. *Appl*. *Cryst*., 2009, **42**, 339.
33. L. J. Bourhis, O. V. Dolomanov, R. J. Gildea, J. A. K. Howard, and H. Puschmann, *Acta Cryst*., 2015, **A71**, 59.
34. G. M. Sheldrick, *Acta Cryst*., 2015, **C71**, 3.
35. Q. Hu, C. Qin, L. Huang, H. Wang, Q. Liu, and L. Zeng, *Dyes Pigm*., 2018, **149**, 253.
36. F. Wu, Y. Zhang, L. Huang, D. Xu, and H. Wang, *Anal*. *Methods*, 2017, **9**, 5472.